Accepted Manuscript

Innervation changes induced by inflammation in the murine vagina

Harman Sharma, Esther Ji, Pauline Yap, Pat Vilimas, Melinda Kyloh, Nicholas Spencer, Rainer Viktor Haberberger, Christine M. Barry

Please cite this article as: H. Sharma, E. Ji, P. Yap, P. Vilimas, M. Kyloh, N. Spencer, R. Viktor Haberberger, C.M. Barry, Innervation changes induced by inflammation in the murine vagina, *Neuroscience* (2017), doi: https://doi.org/10.1016/j.neuroscience.2017.12.026
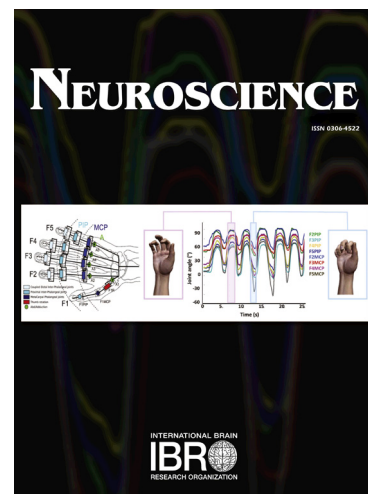
Title

INNERVATION CHANGES INDUCED BY INFLAMMATION IN THE MURINE VAGINA

Authors

Harman Sharma[1]*, Esther Ji[1]*, Pauline Yap[1], Pat Vilimas[1], Melinda Kyloh[2], Nicholas Spencer[2], Rainer Viktor Haberberger[1] and Christine M Barry[1]

*Equal first authors

Affiliations

1. Anatomy and Histology, and Centre for Neuroscience, College of Medicine and Public Health, Flinders University, Adelaide, SA
2. Human Physiology, and Centre for Neuroscience, College of Medicine and Public Health, Flinders University, Adelaide, SA

Corresponding author

Christine Barry

Anatomy and Histology

Flinders University

GPO Box 2100

Adelaide SA 5001

Australia

Email: christine.barry@flinders.edu.au

Tel: + 61 8 8204 5468

Abstract

Vulvodynia is a prevalent chronic pain disorder associated with high medical costs and often ineffective treatments. The major pathological feature is proliferation of vaginal nerve fibres. This study aimed to develop a highly reproducible animal model to study neuroproliferation in the vagina and aid the identification of appropriately targeted treatments for conditions such as vulvodynia. Mild chronic inflammation was induced using microinjection of complete Freund's adjuvant in the distal vagina of C57Bl/6 mice. Control mice received saline. Inflammation and innervation density were assessed at 7 and 28 days after a single administration or 14 days following repeated administration of complete Freund's adjuvant or saline. Histochemistry and blinded-analysis of images was used to assess vaginal morphology (H & E) and abundance of macrophages (CD68-labelling), mast cells (toluidine blue staining, mast cell tryptase-immunoreactivity), blood vessels (αSMA-immunoreactivity) and nerve fibres immunoreactive for the pan-neuronal marker PGP9.5. Subpopulations of nerve fibres were identified using immunoreactivity for calcitonin gene-related peptide (CGRP), substance P (SP), vasoactive intestinal peptide (VIP) and neuropeptide Y (NPY). Single administration of complete Freund's adjuvant resulted in vaginal swelling, macrophage infiltration, vascular proliferation and increased abundance of nerve fibres immunoreactive for CGRP, SP, VIP and/or PGP9.5 but not NPY, evident at seven days. Inflammation further increased following repeated administration of complete Freund's adjuvant but nerve fibre proliferation did not. Nerve fibre proliferation continued to be evident at 28 days. The inter-individual differences within each treatment group were small, indicating this model may be useful to study mechanisms underlying vaginal nerve fibre proliferation associated with inflammation.

Introduction

Vulvodynia is a prevalent chronic pain disorder of the distal female reproductive tract with unclear aetiology (Pukall et al., 2016). Clinical signs include evidence of nociceptor sensitisation (Bohm-Starke et al., 2001) and pathological features include increased numbers of vaginal nerve fibres (Bohm-Starke et al., 1998, Tympanidis et al., 2003, Goetsch et al., 2010, Liao et al., 2017), possibly resulting from inflammation (Akopians and Rapkin, 2015, Liao et al., 2017). Treatments for vulvodynia include topical and systemic medications, physical therapy, sexual counseling and surgery, but these are often ineffective (Harlow et al., 2014). Direct medical costs are high, exceeding $21 billion annually in the United States (Xie et al., 2012). Current understanding of the processes underlying neuroproliferation in response to vaginal inflammation is limited.

Vaginal innervation includes projections of sympathetic, parasympathetic and sensory neurons. Many nerve fibres in the vagina contain peptides such as vasoactive intestinal polypeptide (VIP), calcitonin gene-related peptide (CGRP), substance P (SP) and neuropeptide tyrosine (NPY) that regulate blood flow and nociception (Huang et al., 1984, Hoyle et al., 1996). The types of nerve fibres contributing to hyperinnervation in vulvodynia are largely unknown.

Hyperinnervation of synovium and skin has been shown in mouse models of joint and hind paw inflammation, induced using complete Freund's adjuvant (CFA) (Ghilardi et al., 2012, Chakrabarty et al., 2013). CFA is comprised of heat-inactivated mycobacterium emulsified in mineral oil and the gradual release of antigens from the suspension produces a sustained immune response, making CFA useful in models of chronic inflammation (Billiau and Matthys, 2001) (Su et al., 2005). To our knowledge CFA has not previously been used in studies of the female genital tract and the impact of mild chronic inflammation on the innervation pattern of peptidergic nerve fibres in the vagina is unclear.

Therefore this study aimed to investigate the impact of mild chronic inflammation induced by CFA on innervation of the murine vagina. We focused on nerve fibres containing VIP, CGRP, SP and NPY due to their recognised actions in inflammation and nociception.

Methods

General procedures

All experiments were performed according to the guidelines established by the National Health and Medical Research Council of Australia and were approved by the Animal Welfare Committee of Flinders University.

Induction of inflammation

Under general anaesthesia with isoflurane (induction 4%, maintenance 1.5%) in oxygen, female mice (C57Bl/6 6 to 8 weeks of age, independent of the oestrus cycle) received injection of CFA (Sigma-Aldrich, Missouri, USA) into the wall of the distal vagina. Control mice were injected with 0.9 % saline using the same procedures. To optimize the injection procedure, pilot studies (n = 3 mice) were undertaken in which 5 μl of Evan's blue dye (5% in 0.9% saline) was injected into the distal vaginal wall and dissection performed immediately afterwards to confirm the distribution of dye. To minimize trauma to the mucosa, injection was administered using a glass micropipette (inner diameter: 1.5 mm; World Precision Instruments, FL, USA), which had been pulled on a Flaming Brown micropipette puller (Sutter Instrument Co. CA, USA) to produce a tip diameter of approximately 5 μm and a custom-made pressure injection system (Biomedical Engineering, Flinders University) was used to inject 5 μl of solution. To visualize the distribution of injected substances during the procedure, a small quantity of Evan's blue dye (5%) was included in injected solutions. Following injection, anaesthesia was withdrawn and mice recovered. Following the procedure all mice were monitored at least twice daily for any evidence of pain or distress, including weight loss, exploratory behaviour deficits, licking or biting response to urogenital tract inflammation, piloerection and facial grimace scale (Langford et al., 2010). After 7 days mice were either euthanized by isoflurane overdose and heart removal (CFA 7d n = 7, Saline 7d n = 4), or anaesthetized again and administered a second time with CFA or saline using the same procedures described previously. These mice were then allowed to recover for a further 7 days with monitoring as previously described and then euthanized by isoflurane overdose and heart removal (CFA 14d n = 6, Saline 14d n = 4). An additional group of mice were euthanized at 28 days following a single administration of CFA (CFA 28d, n = 4) or saline (Saline 28d, n = 2).

Tissue preparation and sectioning

Tissue sections were used to assess the presence of inflammation and to semi-quantitate nerve fibres distributed in different layers of the murine vagina in proximal (cervical) and distal (vulvar) segments. Following euthanasia, the vagina together with the urethra was dissected and proximal and distal segments isolated (Fig. 1A). Tissue was fixed overnight at 4°C in Zamboni's fixative (2% formaldehyde; 0.5% picric acid; 0.2M sodium phosphate buffer, pH 7.0), then dehydrated in ethanol (80% 3 x 20 min, 90% 1 x 30 min, 100% 2 x 30 min), cleared in xylene (2 x 30 minutes) and rehydrated through a series of ethanol washes (100% 2 x 30 min, 80% 1 x 30 min, 50% 1 x 30 min) to water (1 x 30 min). Tissue was transferred into 30% sucrose in PBS overnight at 4°C then shock frozen in OCT compound (Tissue-Tek, Miles, USA). Cryostat sections were cut at 12 µm thickness, mounted on polyethyleneimine-coated slides and vacuum dried for 30 minutes. For each histological stain and each combination of antibodies, five sections from the proximal and five sections from the distal segment of the vagina per mouse were labelled, with at least 100 µm distance between sections labelled with the same stain or antibody combination.

Histochemistry

Haematoxylin and eosin (H&E) staining was used to visualise vaginal tissue morphology following microinjection of CFA or saline. Sections were washed in PBS and stained according to standard protocols (haematoxylin 45 s, 1% acid alcohol 5 s, lithium carbonate 1 min, eosin 5 – 7 s, 100% ethanol 3 x 10 s and xylene 2 x 1 min). Sections were washed under running water (1 min) after immersion in each reagent before dehydration in ethanol. Slides were coverslipped using DePex mounting medium (BDH Chemicals, Poole, UK).

Toluidine blue staining was performed to identify mast cells in the vagina following microinjection of CFA or saline. Slides were washed in PBS to remove OCT, subsequently toluidine blue working solution (1%) was applied for 5 min, sections washed again in PBS then coverslipped in carbonate-buffered glycerol at pH 8.6. Multiple labelling immunohistochemistry was used to identify specific populations of nerve fibres, CD68 immunoreactive cells, mast cells and blood vessels containing alpha-smooth muscle actin (αSMA). Non-specific binding was blocked using 10% normal donkey serum in PBS (30 minutes), and sections were incubated in primary antisera

(Appendix, Table A.1) for 48 hours in a humid chamber at room temperature. Combinations of primary antisera are also listed in the appendix table. The pan-neuronal marker protein gene product 9.5 (PGP9.5) was used to identify all nerve fibres, and subpopulations of fibres were identified by immunoreactivity for SP, CGRP and VIP. Alpha-smooth muscle actin was used to identify blood vessels. The monocyte/macrophage marker CD68 was used to assess the presence of macrophages and histamine was used as a marker of mast cells. After exposure to primary antisera, sections were washed in PBS (3 x 10 min), incubated in combinations of secondary antisera (Table A.1) for 2 hours at room temperature, washed in PBS (3 x 10 min) and coverslipped in carbonate-buffered glycerol at pH 8.6.

Antibody characterisation

Primary antibodies and antisera used in this study are summarised in the Appendix (Table A.1). The monoclonal αSMA antibody, produced using a mouse-derived hybridoma (Skalli et al., 1986) labels a 42-43 kD band on Western blot (Yang et al., 2001, Lennerz et al., 2008). The polyclonal CGRP antibody has been extensively characterized in previous studies (Morris et al., 2005b, Clarke et al., 2011, Vilimas et al., 2011, Yuan et al., 2011), shows no cross-reactivity with unrelated peptides in sensory or autonomic ganglia (Gibbins and Matthew, 1996) and exhibits labelling consistent with other reported CGRP antibodies (Gibson et al., 1984, Franco-Cereceda et al., 1987). The polyclonal PGP9.5 antibody (Doran et al., 1983) labels a band at 26 – 28 kD on Western blot (Krimm et al., 2006, Van Acker et al., 2016), and labels neurons and nerve fibres of peripheral and central nervous system and some neuroendocrine cells (Wilson et al., 1988). The monoclonal SP antibody (Millipore), produced using a hybridoma (Cuello et al., 1979) has shown specificity in radioimmunoassay using recombinant substance P or tissue extracts (Cuello et al., 1979). This antibody strongly labels the substantia gelatinosa of the spinal cord (Cuello et al., 1979) and a subset of peripheral nerve terminals in skin and viscera of mice and guinea pigs (Morris et al., 2005a). We have previously shown specificity of the polyclonal VIP antibody using pre-adsorption studies (Morris et al., 1985). No labelling was seen when preparations were treated only with secondary antisera.

Microscopy and image analysis

Sections stained for haematoxylin and eosin (H&E) were viewed using brightfield microscopy (Olympus BX50) and images acquired using a 4 x objective lens. To assess the impact of oedema associated with inflammation on the dimensions of the vaginal wall, the cross-sectional area of the lamina propria was measured using the freehand selection tool and measure function in ImageJ. Sections stained for toluidine blue were viewed with brightfield microscopy using a 20 x objective lens and the number of mast cells per 200,000 μm^2 field was counted in each section.

Immuno-labelled sections were imaged using an epifluorescence microscope (Olympus BX50, Tokyo, Japan) with selective excitation LED (CoolLED Ltd, Hampshire, UK) and emission filter combinations. Images were acquired using a CoolSNAP fx monochromatic camera (Photometrics, Az, USA) and MicroManager Imaging Software (UCSF, Ca, USA). CD68-immunolabelled cells in 6 regions of interest per mouse were imaged using a 20 x objective lens. Images were imported to ImageJ (NIH, Bethesda, MD, USA) and a 9 x 7 point grid was overlaid using the digital Grid tool. CD68-immunoreactive cells intersecting with points on the grid were manually counted, by a researcher blinded to the treatment group, according to techniques previously validated (Gibbins et al., 2003, Gibbons et al., 2010). To compare the number of blood vessels showing immunoreactivity for αSMA in each group, 3 regions per section (30 regions of interest per mouse) were imaged using a 10 x objective lens. The number of αSMA-immunoreactive blood vessels per field was counted for n = 6 mice per group that received injections of CFA and n = 3 mice per group that received injections of saline. To compare the number of immunoreactive nerve fibres in each group, images were acquired from three regions per section (Fig. 1B) using a 20 x objective lens. Thirty regions of interest per mouse were imaged for naiive, CFA 7d, Saline 7d, CFA 14d and Saline 14d groups. Eighteen regions of interest per mouse were imaged for CFA 28d and Saline 28d groups. Images were imported to ImageJ (NIH, Bethesda, MD, USA) and a 9 x 7 point grid was overlaid using the digital Grid tool. Immunoreactive nerve fibres intersecting with points on the grid were manually counted by researchers blinded to the treatment group.

High-resolution images of immunolabelled sections were acquired using a confocal laser scanning microscope (TCS SP5, Leica, Bensheim, Germany) with Leica Application

Suite Advanced Fluorescence software (Leica Microsystems, Wetzlar, Germany) and oil-immersion objective lenses. Images were prepared for publication using Adobe Photoshop (V14.2) and Adobe Illustrator (V17.1).

Statistical analysis

For parametric tests, normal distributions and the equality of group variances were assessed using Shapiro-Wilk tests and Levene's test in SPSS (V23 Armonk, NY, IBM Corp.), and no deviations from normality or differences in variance were shown. Data were analysed in GraphPad Prism (Graphpad Software V6, San Diego), using analysis of variance (ANOVA) followed by Bonferroni post-tests, and are displayed as mean ± standard error of the mean. The relationship between outcome measures was assessed using the Pearson product-moment correlation coefficient. A p value < 0.05 is considered significant.

Results

Overview

Pilot studies showed injected solutions spread throughout the distal vagina and dispersed towards the proximal vagina (data not shown). There was no leakage into adjacent viscera or into the peritoneal space. No physical damage was apparent when fine micropipette tips were impaled into or retracted from the vagina in vivo, as observed using a surgical/dissection microscope. Following injection of CFA or saline, the mice showed no evidence of pain or distress throughout the monitoring period, except a small proportion (< 10%) that demonstrated licking of the urogenital region for 5 to 10 seconds only during recovery from anaesthesia following injection of CFA. Mice injected with CFA showed lamina propria thickening, increased presence of CD68-immunoreactive cells, increased abundance of blood vessels and increased nerve fibre density, including increased numbers of nerve fibres immunoreactive for CGRP, SP and VIP.

Morphological evidence of oedema

CFA produced swelling of the vagina, shown by increased cross sectional area (Fig. 1 C, D). Lamina propria area was significantly increased at 7 days following a single CFA administration ($F_{1, 6}$ = 34.8, p < 0.01) and at 14 days, following repeated CFA administration ($F_{1, 6}$ = 504.0, p < 0.001, Fig. 2A), compared to mice that received saline. Swelling was greater in mice that received two administrations of CFA (CFA 14d group) compared to mice that received a single administration (CFA 7d group, $F_{1, 8}$ = 151.5, p < 0.0001), and was greater in the distal compared to the proximal vagina (CFA 7d vs Saline 7d, $F_{1, 6}$ = 145.0, p < 0.0001; CFA 14d vs Saline 14d, $F_{1, 6}$ = 402.1, p < 0.0001). In control groups of mice, lamina propria area was the same in proximal and distal segments of the vagina. At 28 days following CFA, swelling in the distal vagina was no longer evident (Fig. 2A).

Immune cell infiltration

Vaginal tissue contained an increased number of CD68-immunoreactive cells following a single administration of CFA compared to saline ($F_{1, 7}$ = 312.7, p < 0.0001, Fig. 2B). Repeated administration of CFA produced a further increase in CD68-immunoreactive cells ($F_{1, 5}$ = 2302, p < 0.0001), where as in control mice, the number of CD68-immunoreactive cells was the same in 7d and 14d groups. Mice that received CFA had more abundant CD68-immunoreactive cells in the distal vagina compared to the

proximal vagina (CFA 7d, $F_{1, 7}$ = 100.7, p < 0.0001; CFA 14d, $F_{1, 5}$ = 162.4, p < 0.0001) whereas control mice had the same number of CD68-immunoreactive cells in the proximal and distal vagina. In contrast to changes involving the number of CD68-immunoreactive cells in the vagina, mast cells visualized by toluidine blue staining or by immunoreactivity to histamine were equally abundant in mice that received CFA or saline with only 1 to 2 mast cells per 200,000 μm^2 field identified in all groups of mice.

Vascular proliferation

More blood vessels identified by αSMA-immunoreactivity of the tunica media were identified in mice that received a single ($F_{1, 7}$ = 22.5, p < 0.01) or repeated administration of CFA ($F_{1, 7}$ = 37.1, p < 0.001) compared to mice that received saline (Fig. 2C). Compared to CFA 7d mice, CFA 14d mice showed no further increase in blood vessel numbers identified by αSMA. Whereas mice that received saline showed the same number of αSMA-immunoreactive blood vessels in the distal and proximal vagina, mice that received CFA tended to have more vessels identified by αSMA in the distal vagina.

Innervation density

In all groups of mice, independent of treatment, innervation density was greater in the proximal compared to the distal vagina ($F_{1, 11}$ = 33.9, p = 0.0001, Fig. 2D). Saline administration caused no change in innervation density compared to naïve mice, whereas innervation increased in mice that received CFA (Fig. 2D, 3). Seven days following a single administration of CFA, the number PGP9.5-immunoreactive nerve fibres per field was higher in proximal and distal segments compared to naiive and saline control mice ($F_{2, 11}$ = 57.2, p < 0.0001). CFA 14d mice showed increased innervation in the proximal vagina compared to Saline 14d mice and naiive mice ($F_{2, 11}$ = 11.6, p = 0.002, Fig. 2D). Compared to a single administration of CFA (CFA 7d group), no further increase in innervation density was identified following repeated administration (CFA 14d group). CFA 28d mice showed increased innervation compared to naiive mice ($F_{1, 6}$ = 8.7, p = 0.03, Fig. 2D), with increased innervation density in proximal and distal segments of the vagina similar to other mice treated with CFA. Innervation density in the distal vagina of CFA 14d mice could not be reliably assessed due to substantial oedema and many fields containing sparse tissue and few identifiable nerve fibres. Comparing the impact of CFA on the number of PGP9.5-immunoreactive nerve fibres in proximal and distal segments of the vagina in CFA 7d mice, a more

pronounced response appears in the distal segment. Innervation density in the proximal vagina increased by 44% in mice that received CFA compared to saline (Saline 7d: mean total 40 ± 1 fibres per segment, n = 4; CFA 7d: 57 ± 3, n = 6) whereas in the distal vagina, innervation density increased by over 50% in mice that received CFA compared to saline (Saline 7d: 30 ± 2, n = 4; CFA 7d: 46 ± 2, n = 6). Neither CFA 7d mice nor CFA 14d mice showed any correlation between segmental innervation density and the number of CD68 cells, the number of αSMA-blood vessels or the cross-sectional area of the lamina propria.

Neurochemical characteristics of nerve fibres

In all mice, nerve fibres immunoreactive for CGRP, SP or VIP were most abundant in the lamina propria layer of the vagina whereas nerve fibres immunoreactive for NPY were mainly restricted to the adventitia and muscularis. Compared to saline controls, vaginal sections from CFA 7d mice contained significantly more nerve fibres immunoreactive for CGRP ($F_{1, 16}$ = 29.2, p < 0.0001, Fig. 4A), SP ($F_{1, 16}$ = 15.6, p < 0.01, Fig. 4B) and VIP ($F_{1, 16}$ = 10.1, p < 0.01, Fig. 4C). Repeated administration of CFA produced no further increase in nerve fibres immunoreactive for any of these peptides. Comparing proximal and distal segments, the proximal vagina showed a greater increase in innervation by nerve fibres immunoreactive for CGRP ($F_{1, 16}$ = 6.3, p < 0.05, Fig. 4D). Post-tests showed that in the proximal vagina, innervation by nerve fibres immunoreactive for SP and VIP was also increased (Fig. 4E, F). We did not identify proliferation of nerve fibres containing NPY and in mice that received CFA. NPY-immunoreactive fibres remained mostly restricted to the outer layers of the vagina.

For all mice there was a positive correlation between the number of nerve fibres immunoreactive for PGP9.5 and for CGRP (r = 0.95, p < 0.0001). In contrast, there was no correlation between the number of fibres of any specific immunoreactivity assessed and the number of CD68 cells, the number of blood vessels identified by αSMA or the cross-sectional area of the lamina propria.

Discussion

This study shows that microinjection of CFA induces inflammation and hyperinnervation in the mouse vagina. A single administration of CFA produced oedema, influx of macrophages and proliferation of blood vessels and nerve fibres, all evident after 7 days. Repeated administration of CFA produced greater oedema, macrophage influx and abundance of blood vessels, but no change in the density of nerve fibres. The increased number of nerve fibres was not restricted to one population but involved multiple, neurochemically distinct types of neurons. The nerve fibre proliferation was not coupled to overt pain behaviour since throughout the study, mice showed no signs of pain or distress, consistent with mild chronic inflammation as opposed to severe acute inflammation.

The increase in the area of the lamina propria following CFA administration is consistent with vaginal swelling due to vasocongestion and oedema, increased water content in tissues. Not surprisingly, swelling was more prominent in the distal vagina, closer to the site of CFA administration, and CFA 7d mice showed swelling in the distal vagina only. Greater swelling followed repeated administration of CFA, and CFA14d mice showed swelling of both segments. For this group, lamina propria area in the distal vagina increased over 2.5 fold compared to sham mice, whilst a more modest increase, less than 20%, was seen in the proximal vagina. Despite the substantial oedema produced in response to CFA, animal-to-animal variation within each group was surprisingly small. This points towards an advantageous model. Studies in CFA-induced inflammation in other tissues also reported a robust inflammatory response to CFA with marginal animal-to-animal variation, e.g. 50% increase in mouse hind paw volume at 24 hours, maintained at 7 days following intra-plantar injection of CFA (20 µl), (Cobos et al., 2012).

Infiltration of immune-competent cells is a hallmark of inflammation and cells labelled for CD68 were more numerous in vaginal tissue of mice that received CFA. CD68 is a transmembrane glycoprotein expressed by cells of monocyte lineage (Holness and Simmons, 1993). It is most commonly used as a marker for macrophages, which play key roles in inflammation production and resolution (Fujiwara and Kobayashi, 2005). CD68-immunoreactive cell counts were higher following repeated administration of CFA compared to a single administration, and cell counts were higher in the distal compared to the proximal vagina. Not surprisingly, vaginal tissue that received the highest

exposure to the pro-inflammatory stimulus contained the highest number of CD68-immunolabelled cells. CD68 cell infiltration appears to be a relatively sensitive measure of inflammation; no oedema was identified in the proximal vagina of CFA 7d mice yet this region contained 80% more CD68-labelled cells compared to controls. Our results are consistent with previous studies that have identified macrophage infiltration in CFA models of hind paw inflammation (Jha et al., 2014) and joint inflammation (Ghilardi et al., 2012). The results in our model corroborate patient studies that identified increased numbers of CD68-labelled cells in vestibular biopsies of women with vestibulodynia, a localized form of vulvodynia involving pain associated with the vaginal vestibule (Liao et al., 2017). Thus, infiltration of CD68-positive cells is present in human pathology and in this proposed animal model.

Mast cells are also often associated with inflammation but, in contrast to increased putative macrophages in vaginal tissue following administration of CFA, there was no increase in mast cells. This was confirmed by two methods to identify mast cells, which yielded equivalent results. Resident mast cells are part of the innate immune system and release mediators that contribute to nociceptor sensitisation (Drummond, 2004, Ren and Dubner, 2010). Mast cell accumulation in vulvar tissue has been described in a mouse model of oxazolone induced hypersensitivity, concurrent with hyperinnervation involving CGRP-immunoreactive nerve fibres (Landry et al., 2017). The results of clinical studies are variable. In women with provoked vestibulodynia, pathology regarding increased presence of mast cells is variable (Chalmers et al., 2016). Mediators released by mast cells can contribute to sensitisation and proliferation of peripheral nociceptors and a potential limitation of our model relates to its utility for studies into mechanisms involving mast cells that may contribute to vulvodynia. Whilst the significance of mast cells in vaginal hyperinnervation and nociceptor sensitization in vulvodynia remains unclear, our model provides evidence that hyperinnervation can occur independent of changes in mast cell numbers. Recent studies using a rat model of CFA-induced vulvodynia indicate an important role for macrophages and T cells, via increased renin and angiotensinogen leading to promotion of axonal sprouting through AT2 receptor activation (Chakrabarty et al., 2017).

Substantial vascular proliferation was observed in vaginal tissue of mice that received CFA. After a single administration, a 2-fold increase in αSMA-labelled blood vessels was

identified in the distal vagina. After repeated administration of CFA, the number of blood vessels further increased in both segments of the vagina. Consistent with findings regarding swelling and macrophage infiltration, vascular proliferation was greater in the distal vagina, but was also substantial in the proximal vagina which contained more than double the number of αSMA-vessels after repeated CFA administration. As αSMA-labelling selectively identifies arterioles and other vessels containing smooth muscle, the 2- to 3-fold increase in the number of vessels identified is a conservative measure of total vascular proliferation as capillaries which do not show αSMA-immunoreactivity are more abundant. Angiogenesis is a key response to tissue insult and vessel proliferation is rapid (DiPietro, 2016). Endothelial cell proliferation in tracheal microvasculature has been shown within 24 hours of inoculation with Mycoplasma pulmonis, peaking at 5 days, though remaining elevated for 28 days compared to control mice (Ezaki et al., 2001). Our data is also consistent with experimental studies showing CFA-induced endothelial cell proliferation in mouse synovium (Ghilardi et al., 2012). Furthermore, clinical studies show patients with rheumatoid arthritis have increased vessels labelling for αSMA, and the increase correlates with ultrasound measures of joint disease severity (Kelly et al., 2015). An interesting question is whether hyperinnervation associated with vulvodynia mainly involves perivascular nerve fibres. It has been shown that many nociceptive afferents in health tissues are perivascular (Gibbins et al., 1985). Interestingly, our search of the literature found no reports of vascular proliferation in vaginal biopsies from women with vulvodynia, and one study reported vascular proliferation was not evident in haematoxylin and eosin labelled samples from women with vestibulitis (Halperin et al., 2005). The presence and potential significance of angiogenesis in vulvodynia requires clarification.

Hyperinnervation in vaginal biopsies is the major pathological feature associated with vulvodynia (Bohm-Starke et al., 1998, Tympanidis et al., 2003, Halperin et al., 2005, Leclair et al., 2011, Liao et al., 2017). In our model, a single administration of CFA produced substantial hyperinnervation involving both segments and therefore the entire length of the mouse vagina. Surprisingly, no further increase in innervation was identified following a second administration of CFA. However, it should be noted that the accuracy of innervation density measurement in CFA 14d mice could have been limited by the substantial oedema in this group. An association between hyperinnervation and increased mechanical sensitivity has been demonstrated in the repeated fungal infection

model of vulvodynia, in which mice with vaginal hyperinnervation demonstrate mechanical allodynia (Farmer et al., 2011). In the fungal infection model of vulvodynia, mechanical allodynia was demonstrated to persist after resolution of acute inflammation. In contrast to the fungal infection model, the present study describes a model of vaginal hyperinnervation, not vulvodynia, as altered pain sensitivity cannot be inferred. The consistent hyperinnervation response to CFA and limited animal-to-animal variation identified in the present study is similar to the consistent hyperinnervation response identified in CFA models of hind paw and joint inflammation (Ghilardi et al., 2012, Chakrabarty et al., 2013). This supports the view that CFA administration can provide a robust model to study vaginal hyperinnervation. Any studies utilizing this model must recognise that dispersion of CFA can result in inflammation and hyperinnervation not confined to the injection site.

Using multiple labelling we investigated if hyperinnervation was restricted to specific nerve fibre populations. We found multiple populations of fibres contributed to hyperinnervation in response to CFA. CGRP-immunoreactive, SP-immunoreactive and VIP-immunoreactive nerve fibres were all more abundant, as were nerve fibres identified by PGP9.5 and not labelling for any peptide investigated. In contrast, proliferation of nerve fibres containing the peptide NPY was not evident following administration of CFA. Our finding regarding proliferation of CGRP-containing nerve fibres is consistent with that shown in the oxazolone hypersensitivity model of vulvodynia (Landry et al., 2017), and proliferation of CGRP-containing nerve fibres identified in a subset of mice (40%) that demonstrated hyperalgesia in the repeated fungal infection model of vulvodynia, following three rounds of *candida albicans* infection (Farmer et al., 2011). Further work is required to precisely identify the origin of nerve fibres, however it has been shown that CGRP- and SP- containing nerve fibres in the mouse vagina are associated with lumbar and sacral DRG, and these peptides are not found in autonomic ganglion neurons associated with the vagina (Jobling and Lim, 2008, Vilimas et al., 2011, Barry et al., 2017).

In addition to proliferation of CGRP- and SP-containing nerve fibres, proliferation of VIP-containing fibres was identified following administration of CFA. Proliferation of VIP-containing nerve fibres has previously been shown in a rat model of colitis (Miampamba and Sharkey, 1998) and further investigation is warranted to identify the role and origin

of these fibres. VIP is a potent vasodilator, known to increase vaginal blood flow and lubrication (Ottesen et al., 1987). Anti-inflammatory effects of VIP have been shown in animal models and in vitro studies (Chedid et al., 2017). The mouse vagina contains multiple populations of VIP-immunoreactive nerve fibres, including projections of sensory and autonomic neurons (Costa et al., 1988, Barry et al., 2017). Further studies are required to determine if VIP-containing postganglionic projections of pelvic ganglion neurons contribute to vaginal hyperinnervation.

An important question is does vaginal hyperinnervation in this model reflect hyperinnervation seen in patients? Neurochemical characterization of nerve fibres in vaginal biopsies from women with vulvodynia is limited. Increased CGRP-containing nerve fibres (Bohm-Starke et al., 1999) and fibres expressing TRPV1 (Tympanidis et al., 2004) and TRPV4 (Liao et al., 2017) have been identified. TRPV1 receptors are activated by multiple mechanical and chemical stimuli and are mainly found in nociceptors, including many DRG neurons containing both SP and CGRP (Price and Flores, 2007). TRPV4 receptors contribute to mechano-nociception and are found in a subset of CGRP-immunoreactive nerve fibres (Brierley et al., 2008). Therefore initial results indicate increased innervation by CGRP and SP containing fibres in this model may reflect aspects of axonal proliferation in women with vulvodynia.

In summary, microinjection of CFA in the distal vagina of mice produced swelling, macrophage infiltration, vascular proliferation and vaginal hyperinnervation involving multiple types of nerve fibres. Repeated injection of CFA produced greater inflammation without increasing innervation. Inflammation was greater in the distal compared to the proximal vagina, whereas hyperinnervation was more prominent in proximal vagina, and involved CGRP-, SP- and VIP-immunoreactive nerve fibres, in addition to nerve fibres not labelling for any of these peptides. The highly reproducible innervation changes in response to CFA indicate this model may be useful for studies investigating mechanisms underlying hyperinnervation.

References

Akopians AL, Rapkin AJ (2015) Vulvodynia: The Role of Inflammation in the Etiology of Localized Provoked Pain of the Vulvar Vestibule (Vestibulodynia). Semin Reprod Med 33:239-245.

Barry CM, Ji E, Sharma H, Beukes L, Vilimas PI, DeGraaf YC, Matusica D, Haberberger RV (2017) Morphological and neurochemical differences in peptidergic nerve fibers of the mouse vagina. J Comp Neurol.

Billiau A, Matthys P (2001) Modes of action of Freund's adjuvants in experimental models of autoimmune diseases. J Leukoc Biol 70:849-860.

Bohm-Starke N, Hilliges M, Brodda-Jansen G, Rylander E, Torebjork E (2001) Psychophysical evidence of nociceptor sensitization in vulvar vestibulitis syndrome. Pain 94:177-183.

Bohm-Starke N, Hilliges M, Falconer C, Rylander E (1998) Increased intraepithelial innervation in women with vulvar vestibulitis syndrome. Gynecol Obstet Invest 46:256-260.

Bohm-Starke N, Hilliges M, Falconer C, Rylander E (1999) Neurochemical characterization of the vestibular nerves in women with vulvar vestibulitis syndrome. Gynecol Obstet Invest 48:270-275.

Brierley SM, Page AJ, Hughes PA, Adam B, Liebregts T, Cooper NJ, Holtmann G, Liedtke W, Blackshaw LA (2008) Selective role for TRPV4 ion channels in visceral sensory pathways. Gastroenterology 134:2059-2069.

Chakrabarty A, Liao Z, Mu Y, Smith PG (2017) Inflammatory Renin-Angiotensin System Disruption Attenuates Sensory Hyperinnervation and Mechanical Hypersensitivity in a Rat Model of Provoked Vestibulodynia. J Pain.

Chakrabarty A, Liao Z, Smith PG (2013) Angiotensin II receptor type 2 activation is required for cutaneous sensory hyperinnervation and hypersensitivity in a rat hind paw model of inflammatory pain. J Pain 14:1053-1065.

Chalmers KJ, Madden VJ, Hutchinson MR, Moseley GL (2016) Local and Systemic Inflammation in Localized, Provoked Vestibulodynia: A Systematic Review. Obstet Gynecol 128:337-347.

Chedid P, Boussetta T, Dang PM, Belambri SA, Marzaioli V, Fasseau M, Walker F, Couvineau A, El-Benna J, Marie JC (2017) Vasoactive intestinal peptide dampens formyl-peptide-induced ROS production and inflammation by targeting a MAPK-p47phox phosphorylation pathway in monocytes. Mucosal Immunol 10:332-340.

Clarke JN, Anderson RL, Haberberger RV, Gibbins IL (2011) Non-peptidergic small diameter primary afferents expressing VGluT2 project to lamina I of mouse spinal dorsal horn. Mol Pain 7:95.

Cobos EJ, Ghasemlou N, Araldi D, Segal D, Duong K, Woolf CJ (2012) Inflammation-induced decrease in voluntary wheel running in mice: a nonreflexive test for evaluating inflammatory pain and analgesia. Pain 153:876-884.

Costa M, Furness JB, Gibbins IL, Morris JL, Bornstein JC, Llewellyn-Smith IJ, Murphy R (1988) Colocalization of VIP with other neuropeptides and neurotransmitters in the autonomic nervous system. Ann N Y Acad Sci 527:103-109.

Cuello AC, Galfre G, Milstein C (1979) Detection of substance P in the central nervous system by a monoclonal antibody. Proceedings of the National Academy of Sciences of the United States of America 76:3532-3536.

DiPietro LA (2016) Angiogenesis and wound repair: when enough is enough. J Leukoc Biol 100:979-984.

Doran JF, Jackson P, Kynoch PA, Thompson RJ (1983) Isolation of PGP 9.5, a new human neurone-specific protein detected by high-resolution two-dimensional electrophoresis. J Neurochem 40:1542-1547.

Drummond PD (2004) The effect of cutaneous mast cell degranulation on sensitivity to heat. Inflamm Res 53:309-315.

Ezaki T, Baluk P, Thurston G, La Barbara A, Woo C, McDonald DM (2001) Time course of endothelial cell proliferation and microvascular remodeling in chronic inflammation. Am J Pathol 158:2043-2055.

Farmer MA, Taylor AM, Bailey AL, Tuttle AH, MacIntyre LC, Milagrosa ZE, Crissman HP, Bennett GJ, Ribeiro-da-Silva A, Binik YM, Mogil JS (2011) Repeated vulvovaginal fungal infections cause persistent pain in a mouse model of vulvodynia. Science translational medicine 3:101ra191.

Franco-Cereceda A, Henke H, Lundberg JM, Petermann JB, Hokfelt T, Fischer JA (1987) Calcitonin gene-related peptide (CGRP) in capsaicin-sensitive substance P-immunoreactive sensory neurons in animals and man: distribution and release by capsaicin. Peptides 8:399-410.

Fujiwara N, Kobayashi K (2005) Macrophages in inflammation. Curr Drug Targets Inflamm Allergy 4:281-286.

Ghilardi JR, Freeman KT, Jimenez-Andrade JM, Coughlin KA, Kaczmarska MJ, Castaneda-Corral G, Bloom AP, Kuskowski MA, Mantyh PW (2012) Neuroplasticity of sensory and sympathetic nerve fibers in a mouse model of a painful arthritic joint. Arthritis Rheum 64:2223-2232.

Gibbins IL, Furness JB, Costa M, MacIntyre I, Hillyard CJ, Girgis S (1985) Co-localization of calcitonin gene-related peptide-like immunoreactivity with substance P in cutaneous, vascular and visceral sensory neurons of guinea pigs. Neuroscience letters 57:125-130.

Gibbins IL, Jobling P, Teo EH, Matthew SE, Morris JL (2003) Heterogeneous expression of SNAP-25 and synaptic vesicle proteins by central and peripheral inputs to sympathetic neurons. J Comp Neurol 459:25-43.

Gibbins IL, Matthew SE (1996) Dendritic morphology of presumptive vasoconstrictor and pilomotor neurons and their relations with neuropeptide-containing preganglionic fibres in lumbar sympathetic ganglia of guinea-pigs. Neuroscience 70:999-1012.

Gibbons CH, Illigens BM, Wang N, Freeman R (2010) Quantification of sudomotor innervation: a comparison of three methods. Muscle & nerve 42:112-119.

Gibson SJ, Polak JM, Bloom SR, Sabate IM, Mulderry PM, Ghatei MA, McGregor GP, Morrison JF, Kelly JS, Evans RM, et al. (1984) Calcitonin gene-related peptide immunoreactivity in the spinal cord of man and of eight other species. The Journal of neuroscience : the official journal of the Society for Neuroscience 4:3101-3111.

Goetsch MF, Morgan TK, Korcheva VB, Li H, Peters D, Leclair CM (2010) Histologic and receptor analysis of primary and secondary vestibulodynia and controls: a prospective study. American journal of obstetrics and gynecology 202:614 e611-618.

Halperin R, Zehavi S, Vaknin Z, Ben-Ami I, Pansky M, Schneider D (2005) The major histopathologic characteristics in the vulvar vestibulitis syndrome. Gynecol Obstet Invest 59:75-79.

Harlow BL, Kunitz CG, Nguyen RH, Rydell SA, Turner RM, MacLehose RF (2014) Prevalence of symptoms consistent with a diagnosis of vulvodynia: population-based estimates from 2 geographic regions. American journal of obstetrics and gynecology 210:40 e41-48.

Holness CL, Simmons DL (1993) Molecular cloning of CD68, a human macrophage marker related to lysosomal glycoproteins. Blood 81:1607-1613.

Hoyle CH, Stones RW, Robson T, Whitley K, Burnstock G (1996) Innervation of vasculature and microvasculature of the human vagina by NOS and neuropeptide-containing nerves. Journal of anatomy 188 (Pt 3):633-644.

Huang WM, Gu J, Blank MA, Allen JM, Bloom SR, Polak JM (1984) Peptide-immunoreactive nerves in the mammalian female genital tract. The Histochemical journal 16:1297-1310.

Jha MK, Jeon S, Jin M, Ock J, Kim JH, Lee WH, Suk K (2014) The pivotal role played by lipocalin-2 in chronic inflammatory pain. Exp Neurol 254:41-53.

Jobling P, Lim R (2008) Anatomical and physiological properties of pelvic ganglion neurons in female mice. Auton Neurosci 140:30-39.

Kelly S, Bombardieri M, Humby F, Ng N, Marrelli A, Riahi S, DiCicco M, Mahto A, Zou L, Pyne D, Hands RE, Pitzalis C (2015) Angiogenic gene expression and vascular density are reflected in ultrasonographic features of synovitis in early Rheumatoid Arthritis: an observational study. Arthritis Res Ther 17:58.

Krimm RF, Davis BM, Noel T, Albers KM (2006) Overexpression of neurotrophin 4 in skin enhances myelinated sensory endings but does not influence sensory neuron number. J Comp Neurol 498:455-465.

Landry J, Martinov T, Mengistu H, Dhanwada J, Benck CJ, Kline J, Boo B, Swanson L, Tonc E, Daughters R, Fife BT, Chatterjea D (2017) Repeated hapten exposure induces persistent tactile sensitivity in mice modeling localized provoked vulvodynia. PloS one 12:e0169672.

Langford DJ, Bailey AL, Chanda ML, Clarke SE, Drummond TE, Echols S, Glick S, Ingrao J, Klassen-Ross T, Lacroix-Fralish ML, Matsumiya L, Sorge RE, Sotocinal SG, Tabaka JM, Wong D, van den Maagdenberg AM, Ferrari MD, Craig KD, Mogil JS (2010) Coding of facial expressions of pain in the laboratory mouse. Nat Methods 7:447-449.

Leclair CM, Goetsch MF, Korcheva VB, Anderson R, Peters D, Morgan TK (2011) Differences in primary compared with secondary vestibulodynia by immunohistochemistry. Obstet Gynecol 117:1307-1313.

Lennerz JK, Ruhle V, Ceppa EP, Neuhuber WL, Bunnett NW, Grady EF, Messlinger K (2008) Calcitonin receptor-like receptor (CLR), receptor activity-modifying protein 1 (RAMP1), and calcitonin gene-related peptide (CGRP) immunoreactivity in the rat trigeminovascular system: differences between peripheral and central CGRP receptor distribution. J Comp Neurol 507:1277-1299.

Liao Z, Chakrabarty A, Mu Y, Bhattacherjee A, Goestch M, Leclair CM, Smith PG (2017) A Local Inflammatory Renin-Angiotensin System Drives Sensory Axon Sprouting in Provoked Vestibulodynia. J Pain 18:511-525.

Miampamba M, Sharkey KA (1998) Distribution of calcitonin gene-related peptide, somatostatin, substance P and vasoactive intestinal polypeptide in experimental colitis in rats. Neurogastroenterol Motil 10:315-329.

Morris JL, Gibbins IL, Furness JB, Costa M, Murphy R (1985) Co-localization of neuropeptide Y, vasoactive intestinal polypeptide and dynorphin in non-noradrenergic axons of the guinea pig uterine artery. Neuroscience letters 62:31-37.

Morris JL, Gibbins IL, Jobling P (2005a) Post-stimulus potentiation of transmission in pelvic ganglia enhances sympathetic dilatation of guinea-pig uterine artery in vitro. The Journal of physiology 566:189-203.

Morris JL, Konig P, Shimizu T, Jobling P, Gibbins IL (2005b) Most peptide-containing sensory neurons lack proteins for exocytotic release and vesicular transport of glutamate. J Comp Neurol 483:1-16.

Ottesen B, Pedersen B, Nielsen J, Dalgaard D, Wagner G, Fahrenkrug J (1987) Vasoactive intestinal polypeptide (VIP) provokes vaginal lubrication in normal women. Peptides 8:797-800.

Price TJ, Flores CM (2007) Critical evaluation of the colocalization between calcitonin gene-related peptide, substance P, transient receptor potential vanilloid subfamily type 1 immunoreactivities, and isolectin B4 binding in primary afferent neurons of the rat and mouse. J Pain 8:263-272.

Pukall CF, Goldstein AT, Bergeron S, Foster D, Stein A, Kellogg-Spadt S, Bachmann G (2016) Vulvodynia: Definition, Prevalence, Impact, and Pathophysiological Factors. The journal of sexual medicine 13:291-304.

Ren K, Dubner R (2010) Interactions between the immune and nervous systems in pain. Nat Med 16:1267-1276.

Skalli O, Ropraz P, Trzeciak A, Benzonana G, Gillessen D, Gabbiani G (1986) A monoclonal antibody against alpha-smooth muscle actin: a new probe for smooth muscle differentiation. J Cell Biol 103:2787-2796.

Su SB, Silver PB, Grajewski RS, Agarwal RK, Tang J, Chan CC, Caspi RR (2005) Essential role of the MyD88 pathway, but nonessential roles of TLRs 2, 4, and 9, in the adjuvant effect promoting Th1-mediated autoimmunity. J Immunol 175:6303-6310.

Tympanidis P, Casula MA, Yiangou Y, Terenghi G, Dowd P, Anand P (2004) Increased vanilloid receptor VR1 innervation in vulvodynia. European journal of pain 8:129-133.

Tympanidis P, Terenghi G, Dowd P (2003) Increased innervation of the vulval vestibule in patients with vulvodynia. Br J Dermatol 148:1021-1027.

Van Acker N, Rage M, Sluydts E, Knaapen MW, De Bie M, Timmers M, Fransen E, Duymelinck C, De Schepper S, Anand P, Meert T, Plaghki L, Cras P (2016) Automated PGP9.5 immunofluorescence staining: a valuable tool in the assessment of small fiber neuropathy? BMC Res Notes 9:280.

Vilimas PI, Yuan SY, Haberberger RV, Gibbins IL (2011) Sensory innervation of the external genital tract of female guinea pigs and mice. The journal of sexual medicine 8:1985-1995.

Wilson PO, Barber PC, Hamid QA, Power BF, Dhillon AP, Rode J, Day IN, Thompson RJ, Polak JM (1988) The immunolocalization of protein gene product 9.5 using rabbit polyclonal and mouse monoclonal antibodies. Br J Exp Pathol 69:91-104.

Xie Y, Shi L, Xiong X, Wu E, Veasley C, Dade C (2012) Economic burden and quality of life of vulvodynia in the United States. Curr Med Res Opin 28:601-608.

Yang SP, Woolf AS, Quinn F, Winyard PJ (2001) Deregulation of renal transforming growth factor-beta1 after experimental short-term ureteric obstruction in fetal sheep. Am J Pathol 159:109-117.

Yuan SY, Gibbins IL, Zagorodnyuk VP, Morris JL (2011) Sacro-lumbar intersegmental spinal reflex in autonomic pathways mediating female sexual function. The journal of sexual medicine 8:1931-1942.

Figure captions

Fig. 1

Tissue sampling and H & E stained sections

A) Sections for analysis were taken from proximal (cervical) and distal (vulvar) regions of the vagina. Uh, uterine horn; Bl, bladder. B) Using the urethra for orientation, three regions of interest per section were imaged for quantification of immunoreactive cells, blood vessels and nerve fibres. C, D) Typical H & E stained sections showing general morphology of the vaginal wall including larger lamina propria area in this section from a CFA 14d mouse (D) compared to a saline control (C). U, urethra; L, vaginal lumen; E, epithelium; LP, lamina propria; M/A, muscularis and adventitia. Bar = 500 µm.

Fig. 2

Inflammation and hyperinnervation following administration of CFA

A) Mean lamina propria area in sections of the proximal and distal vagina in CFA 7d, 14d and 28d mice and corresponding control groups. In control mice, lamina propria cross-sectional area was the same in the proximal and distal vagina, and the same in Saline 14d compared to Saline 7d mice. CFA 7d and CFA14d mice showed increased lamina propria area, consistent with swelling. Swelling was maximal in CFA 14d mice in the distal vagina, and returned to baseline levels here at 28 days. B) Mean number of CD68-labelled cells per 200,000 μm^2 field in sections from the proximal and distal vagina. In control mice, the number of CD68-labelled cells was similar in sections from the proximal and distal vagina, and the same in Saline 14d compared to Saline 7d mice, and increased in mice that receive CFA, consistent with macrophage infiltration. C) The mean number of blood vessels per 200,000 μm^2 field identified by labelling for αSMA in CFA 7d mice and 14d mice compared to saline controls. Increases in CFA groups are consistent with vascular proliferation and are most pronounced in in the distal vagina where αSMA-labelled blood vessels were equally abundant in CFA14d and CFA 7d mice. D) The mean number of nerve fibres per 200,000 μm^2 field identified by immunoreactivity for PGP9.5 in vaginal sections of all groups of mice. Innervation density was the same in naiive, Saline 7d and Saline 14d mice. All groups that received CFA showed increased innervation density compared to controls and no differences were identified between CFA 7d, CFA 14d and 28d mice.

Asterisks show where Bonferroni post-tests indicate differences between groups that received CFA and Saline (* $p < 0.05$, ** $p < 0.01$, **** $p < 0.0001$). Hashes show where Bonferroni post-tests indicate differences between groups that received CFA (# $p < 0.05$, # # # # $p < 0.0001$). Cross shows when Bonferroni post-tests indicates differences between CFA and naiive.

Fig. 3

Innervation changes following administration of CFA

Confocal microscopy images (z depth 10 μm) of vaginal sections labeled for αSMA (green) and PGP9.5 (red). A – C) Section from the proximal vagina of a Saline 7d mouse showing nerve fibres present in all layers of the vagina, particularly abundant in the lamina propria. D – F) Section from the proximal vagina a CFA 7d mouse showing increased abundance of nerve fibres, particularly in the lamina propria. a, adventitia; m, muscularis; lp lamina propria; e epithelium. Bar = 50 μm.

Fig. 4

Abundance of vaginal nerve fibres immunoreactive for CGRP, SP and VIP

A – C) Graphs show the mean number of nerve fibres per 200,000 $μm^2$ field in sections of the proximal vagina, immunoreactive (+) for a specific peptide. A) Compared to saline controls (n = 4 per group), mice that received CFA (n = 6 per group) had more nerve fibres immunoreactive for CGRP (ANOVA, $p < 0.0001$). Abundance of these fibres was the same in CFA 14d mice compared to CFA 7d mice. B) Mice that received CFA also had increased density of nerve fibres immunoreactive for SP (ANOVA, $p < 0.05$). C) Nerve fibres immunoreactive for VIP were also increased in mice that received CFA (ANOVA, $p < 0.05$). D – F) Graphs show the mean number of nerve fibres per field immunoreactive for a specific peptide in proximal and distal segments of the vagina of CFA 7d and Saline 7d mice. ANOVA showed increases in the number of nerve fibres immunoreactive for CGRP ($p < 0.0001$), SP ($p < 0.01$) and VIP ($p < 0.01$) in mice that received CFA compared to controls, and for each of these peptides, increased innervation was more prominent in the proximal vagina. Asterisks indicate where Bonferroni post-tests show significance. . * $p < 0.05$, ** $p < 0.01$, *** $p < 0.001$

Antibody	Immunogen	Host, source, catalog
Alpha smooth muscle actin (αSMA)	Synthetic NH2-terminal decapeptide of α-SMA conjugated to keyhole limpet hemocyanin	Mouse, Sigma-Aldrich
Calcitonin gene-related peptide (CGRP)	Rat CGRP conjugated to gamma globulin	Goat, Arnel, USA, 178
Neuropeptide tyrosine (NPY)	Synthetic NPY conjugated to bovine thyroglobulin type II using carbodiimide.	Sheep, Dr Oliver and Australia, E2210
Protein gene product 9.5 (PGP9.5)	Human PGP9.5 purified from human brain	Rabbit, Ultraclone, UK
Substance P (SP)	SP conjugated to bovine serum albumin	Rat, Millipore, Millipore
Vasoactive intestinal polypeptide (VIP)	Porcine VIP conjugated to thyroglobulin	Rat, Dr Murphy, Austr

Primary antibody combinations	Secondary antisera and streptavidin conjugates
αSMA	FITC anti-mouse IgG
PGP9.5	CY3 anti-rabbit IgG
NPY	CY5 anti-sheep IgG
PGP9.5	Biotin anti-rabbit IgG + DTAF-SA
SP	CY3 anti-rat IgG
CGRP	CY5 anti-sheep IgG
PGP9.5	Biotin anti-rabbit IgG + DTAF-SA
VIP	CY3 anti-rat IgG
CGRP	CY5 anti-sheep IgG

Abbreviations: FITC, fluorescine isothiocyanate; Cy, cyanine, DTAF-SA, dichlorotriazinyl aminofluorescein-streptavidin.

Highlights

- Complete Freund's adjuvant was microinjected into the distal vagina of C57Bl/6 mice

- Vaginal swelling and increased macrophages and blood vessels were evident at 7 days and 14 days

- Hyperinnervation was evident at 7, 14 and 28 days and involved multiple types of nerve fibres

- Proximal and distal regions of the vagina contained inflammation and hyperinnervation

- Repeated administration of adjuvant increased inflammation but not hyperinnervation